Check for updates

Graphitizability of Polymer Thin Films: An In Situ TEM Study of Thickness Effects on Nanocrystalline Graphene/Glassy Carbon Formation

C. N. Shyam Kumar,* Clemens Possel, Simone Dehm,
Venkata Sai Kiran Chakravadhanula, Di Wang, Wolfgang Wenzel, Ralph Krupke,
and Christian Kübel*

Polymer pyrolysis has emerged as a versatile method to synthesize graphenoid (graphene like) materials with varying thickness and properties. The morphology of the thin film, especially the thickness, greatly affects the graphitizability and the properties of the graphenoid material. Using in situ current annealing inside a transmission electron microscope (TEM), the thickness-dependent structural evolution of the polymer film with a special focus on thickness effects is followed. At high temperatures, thin samples form large graphene layers oriented parallel to the substrate, whereas in thick samples multi-walled cage-like structures are formed. Moleclar Dynamics (MD) simulations reveal a film thickness of 40 Å below which, the carbonized layers align parallel to the surface. For thicker samples, the orientation of the layers becomes increasingly misoriented starting from the surface to the center. This structural change can be attributed to the formation of bonded multi-layers from the initially unsaturated activated edges. The resulting cage-like structures are stable even during simulated annealing at temperatures as high as 3500 K. An atomistic understanding of the formation of these structures is presented. The results clearly indicate the critical effect of thickness on the graphitizability of polymers and provide a new understanding of the structural evolution during pyrolysis.

1. Introduction

Carbonization of polymers at small length scales has emerged as an easy method to synthesize graphenoid (graphene-like) materials for a number of different technological applications.[1,2] This method provides the flexibility of growing graphenoid materials on different substrates with defined thicknesses and also for patterning to achieve different shapes.[3] Recently, carbonized films with interesting optical, mechanical, and electrical properties have been fabricated by pyrolysis of thin polymer films.[4] The method combines ease of fabrication, control over size, shape, and thickness, and the possibility to tailor the properties by varying the polymer precursor and the carbonization conditions. Since the pyrolysis is catalyst-free, the crystallite growth is limited resulting in crystallite sizes on the order of a few nanometers. The material is commonly referred to as nanocrystalline graphene (ncg) when the resulting

C. N. Shyam Kumar, C. Possel, S. Dehm, V. S. K. Chakravadhanula,
D. Wang, W. Wenzel, R. Krupke, C. Kübel
Institute of Nanotechnology
Karlsruhe Institute of Technology
76021 Karlsruhe, Germany
E-mail: Shyam@nitc.ac.in; christian.kuebel@kit.edu

C. N. Shyam Kumar, R. Krupke, C. Kübel
Department of Materials and Earth Sciences
Technical University Darmstadt
64287 Darmstadt, Germany

C. N. Shyam Kumar
School of Materials Science and Engineering
National Institute of Technology
Calicut 673601, India

C. Possel
Fraunhofer Institute for Chemical Technology ICT
76327 Pfinztal, Germany

D. Wang, C. Kübel
Karlsruhe Nano Micro Facility
Karlsruhe Institute of Technology
76021 Karlsruhe, Germany

C. Kübel
Helmholtz Institute Ulm
Karlsruhe Institute of Technology
76021 Karlsruhe, Germany

thickness is ≈1–2 nm. In contrast, pyrolysis of thick films and bulk polymers results in glassy carbon (gc) and graphite depending on the graphitizability of the polymer precursor.[2,5,6]

The structural evolution of bulk carbon sources during pyrolysis is well-studied and a number of different models have been proposed.[6–9] R. Franklin carried out pioneering studies on the pyrolysis of carbons and classified them as graphitizing and non-graphitizing carbons.[6] Pyrolysis of certain carbon sources results in a complete graphitization, leading to the formation of oriented graphite, resulting in the term graphitizing carbon. On the other hand, some carbon sources will not completely graphitize even when heated to very high temperatures, leading to the formation of non-graphitizing/glassy carbon structures. There has been a strong interest to understand the microstructure of non-graphitizing carbons because of their interesting physico-chemical properties. Based on high-resolution transmission electron microscope (TEM) studies of bulk glassy carbon, Harris et al. proposed a fullerene-related structure for commercial glassy carbon.[9] The model consists of discreet fragments of curved carbon sheets with non-six-membered rings that are randomly dispersed between the hexagons. The model also predicts the presence of completely cage-like structures contributing to the observed low density of the glassy carbon structures. All of these studies have been carried out on bulk glassy carbons. However, the strong recent interest in graphenoid thin films necessitates a detailed understanding of the microstructural evolution during pyrolysis at small length scales and the different factors affecting the resulting structure.

Previous studies have shown the effect of size, shape, and thickness on structural evolution and structure-property correlations during pyrolysis at lower length scales. Pyrolysis of thin films (thickness ≈1–2 nm) results in the formation of in-plane oriented few layers of ncg when heated to temperatures ≈1000 °C.[3,10] These studies indicate the possibility of complete graphitization leading to the formation of graphene at higher temperatures. On the other hand, pyrolysis of thick polymer structures does not show layered growth, but results in a microstructure similar to non-graphitizing glassy carbons.[2,11,12] This is indicating the difference in the microstructural evolution and graphitizability during pyrolysis of polymer precursors with different morphology. To understand these differences, a detailed microstructural characterization during pyrolysis is necessary.

Among the various characterization techniques, TEM has been shown to be a versatile tool to understand the structure of pyrolyzed materials with various sizes, shape, and thicknesses, providing high spatial and temporal resolution. In situ heating, as well as current annealing in TEM, have been used to follow the microstructural evolution and structure-property correlations during pyrolysis of thin film polymer precursors. It has been observed that the growth of graphene layers in these films at higher temperatures is dominated by the migration and merging of graphene nano flakes on top of already graphitized layers. This merging is facilitated by the highly reactive edges of the flakes at high temperatures.[13,14] In thicker regions, there is an indication of misoriented growth leading to structures similar to glassy carbon.[14] In situ current annealing studies have mainly been carried out for graphene,[15–16] thicker amorphous carbon films, and carbon fibers.[16–18] Current annealing of graphene has been reported to reach extremely high temperatures and showed catalyst-free conversion of amorphous carbon to graphene nanoflakes on top of graphene.[15] The transformed nano flakes merged and grew on top of the graphene substrate. However, in situ, current annealing of amorphous carbon fibers has been shown to result in the formation of tubular structures.[19] Initially, graphene nano onions form inside carbon tubes, which transform into a tubular structure at higher bias. This is an example of misoriented growth and the presence of closed cage structure in thick samples.[19] Similar ex situ studies on the current annealing of graphite also showed the formation of bonded bilayers and closed graphitic structures.[20]

While the above-mentioned studies discuss the microstructural evolution during pyrolysis of various polymer films in detail, the effect of the film thickness as a critical parameter influencing the microstructural evolution has not yet been investigated in detail. Therefore, the present work aims at understanding the effect of thickness on the microstructural evolution and graphitzability during pyrolysis of polymer films using a combination of in situ TEM studies as an experimental reference and Moliecular Dynamics (MD) simulations to develop an atomistic understanding of processes leading to the formation of the different microstructures. To enable this, we have developed a novel method to prepare freestanding thin polymer films on top of MEMS-based electro-contacting chips to directly observe the structural evolution at high temperatures during current annealing. With this joined experimental and modeling approach, the study provides novel insights into the critical role of thickness in the structural evolution and graphitizability of polymer films.

2. Experimental Section

2.1. Device Fabrication

Commercially available photoresist Microposit S1805 (Rohm& Haas) was used as the starting material (composition given in Table S1, Supporting Information). The photoresist was diluted with propylene glycol monomethyl ether acetate (PGMEA) (Sigma–Aldrich GmbH), spin-coated onto a Si–SiO$_2$ membrane, and ex situ carbonized until 800 °C for 5 h. Spin coating was done at 8000 rpm for 30 s with a solution ratio of 1:21, which resulted in a polymer thickness of ≈10 nm (the reduction ratio of polymer to carbonized thin film of ≈10: 1) and a final thickness of 1 nm for the carbonized film.[4] The ratio was reduced to 1:8 to make thick samples with a final thickness of ≈10 nm for the carbonized film (polymer thickness ≈100 nm). Electro-contacting chips (Aduro from Protochips Inc.) were used for in situ current annealing. To obtain freestanding films, rectangular holes were drilled between the electrodes in the SiN membrane using focused ion beam milling (**Figure 1**) in a Strata 400 FIB (Thermo Fisher Scientific). The *ex situ* carbonized films were transferred onto the MEMS chip. For the transfer to an Aduro electrical chip, the films were coated with PMMA using spin coating and etched using 5% NaOH solution at 70 °C. The stack consisting of 300 nm PMMA and the ncg film was floated off and cleaned thoroughly by subsequent transfer to pure water. The cleaned stack was fished onto an Aduro chip and the PMMA was dissolved by dipping in acetone for 4 h. The clean thin films were patterned using electron beam lithography to form freestanding films across the electrodes (**Figure 2**).
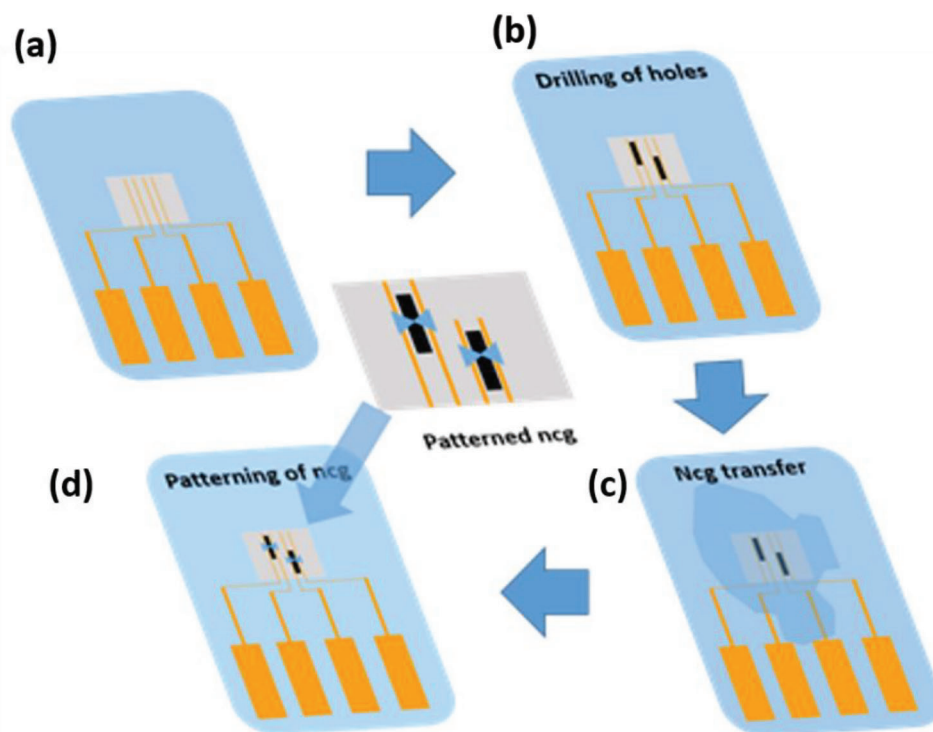
2300230 (2 of 11)

ADVANCED SCIENCE NEWS

www.advancedsciencenews.com

Macro-molecular
Materials and Engineering
Open Access

www.mame-journal.de

Figure 1. Schematic of the sample preparation process. a) MEMS-based Electro-contacting chips (Aduro from Protochips Inc.), b) drilling holes in the freestanding film between the electrodes, c) transferring of the ncg film to the chip, and d) lithographically patterned free-standing ncg across the holes.
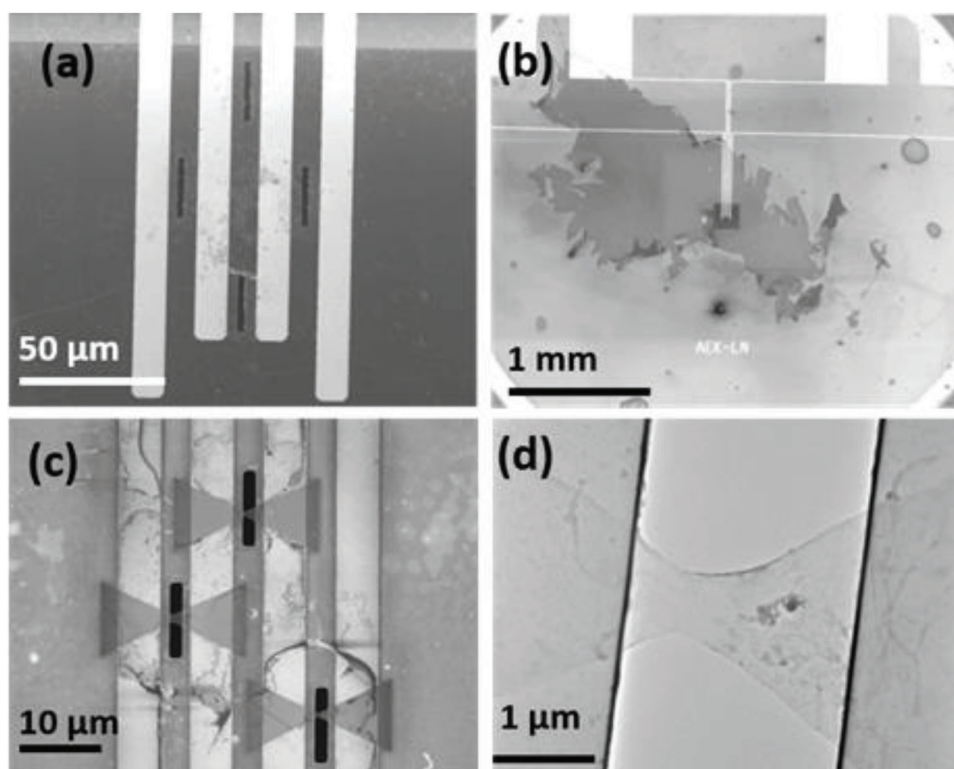

Figure 2. a) Holes drilled between the electrodes of an Aduro chip, b) film transferred across the holes, c) SEM, and d) TEM images of lithographically patterned constrictions across the holes.

For the patterning of the freestanding films, the commercially available negative electron beam resist MaN 2403 (Micro resist technology GmbH) was used to protect the areas to be maintained for the current annealing. The chip was coated with a 300 nm film, heated to 90 °C for 1 min and the required shape was exposed inside an SEM at 30 kV. The exposed film was developed using commercially available AZ 726 MIF (Merck Inc.) for 30 s. The carbonized film was removed using RIE in the unprotected areas and the protective polymer layer was finally removed by dipping in acetone. A constricted shape was chosen so that the region across the holes will have maximum resistance resulting in confined heating in the freestanding region.

By suitably designing freestanding films, heating could be localized, avoiding exposure of the electrodes and support to very high temperatures. In situ current annealing enabled reaching higher temperatures than the commercially available in situ heating setups (1200–1300 °C) and thus provided the possibility to characterize the structural evolution over a wider temperature range. Furthermore, current annealing helps to have a controlled graphinization. Since the nanocarbon material's resistance decreased with increasing graphinization, it was required to impose current annealing by applying current and not voltage. This prevents a thermal runaway and ensures controlled heating since a lower voltage and hence power was required to maintain the current level as the material's resistance decreases progressively. For in situ heating studies, undiluted SU8 (Micro chem) was spin-coated onto a fusion heating chip (Protochips Inc). Spin coating was done at 8000 rpm for 30 s.

2.2. In Situ TEM

TEM analysis was carried out using an aberration-corrected (image) Titan 80-300 TEM (Thermo Fisher Scientific) operated at 80 kV equipped with a US1000 slow scan CCD (Gatan Inc.) camera. Protochips software and control system were used to control the heating current. Initially, the current was increased slowly to observe the stability of the patterned constrictions. At higher current values, a rate of 1 µA s^{-1} was used. Images and SAED patterns were acquired every 100 µA after holding for 5 min. The beam was blanked in between the image acquisition to minimize beam-induced effects. The total time of beam exposure at each temperature varied between 5 and 10 min. In situ heating of SU8 (MicroChem) was carried out using a protochips software and control system as described elsewhere.[13] A heating rate of 10 °C was used with a holding time of 20 min before cooling down. HR imaging was carried out at room temperature.

2.3. MD Simulations

Molecular dynamics simulations were performed with the LAMMPS package using the reactive force field ReaxFF.[21–23] For the simulations, the following protocol was used: first an initial amorphous carbon structure was created with carbon atoms inserted on random positions with a target density of 2 g cm^{-3} (roughly equivalent to the expected equilibrium density of final graphene-like structures). The insertion was done within a specified geometry: 1D periodic structure, 2D thin layer, and 3D bulk structure. In all cases the simulation box used periodic boundary conditions in all directions. It was ensured that the periodic images' interaction could be neglected via adding a vacuum of 15 Å between the periodic images in the structure's desired direction of reduced dimension. Energy minimization was performed to avoid too high overlap of the randomly inserted atoms. Equilibration at room temperature was performed with a time step of 0.2 fs for a time of 20 ps in the canonical ensemble (fixed volume and temperature), yielding an amorphous carbon structure. Then the structure was heated up to 3500 K with the thermostat's damping parameter set to 20 fs and the time step to 0.1 s. In the next step, the dimension of the structure was further reduced during annealing to the desired one (1, 2, and 3D structure) via slicing the structure (i.e., removing particles to get, e.g., a 1D structure from a thin layer). In these cases, the slicing was performed after 100 ps of annealing; afterward, the system was simulated for another 400 ps. In the case of the thin layer, simulation without slicing for an annealing time of 1000 ps was simulated. As a measurement for the alignment of the structures toward the surface, the angle relative to the z-axis (axis perpendicular to the surface) was defined as follows: For each atom I, the three neighboring atoms with (sp^2 hybridized) bonds were determined. From the plane spanned by these three neighboring atoms, the angle of the normal vector relative to the z-axis was determined. In the following, it was referring to this for simplification as the "orientation of the atom". Together with the z position of atom I, this yields the data point for atom i. A detailed view of the number of atoms with more/less than 3 neighbors (e.g., diamond-like sp^3 hybridized bonds with 4 neighbors) showed that their ratio was in the order of 10^{-2} during all simulations carried out for thickness effect evaluation (see also Figure S1, Supporting Information).

3. Results and Discussion

3.1. Structural Evolution during In Situ Current Annealing

The structural evolution during current annealing of a nominally 1 nm thick freestanding film was shown in **Figure 3**. An evolution from a curved and wrinkled structure with very small domains to an ordered structure and subsequent growth of the domains could be seen in the images. The transferred film contained amorphous carbon residues on top of the lithography process. These amorphous carbons transform during current annealing by attaching to the crystallites and/or through a catalyst-free transformation as observed in previous heating studies.[24] The overall structural evolution looks similar to the previously reported evolution during thermal annealing.[14,24] The crystallite size calculated from the intensity profiles of the SAED patterns using the Scherrer formula increases from 2.6 nm at 100 µA to 3.6 nm at 500 µA. The crystallite size of 3.6 nm was slightly >3.2 nm determined for in situ annealed films heated to 1200 °C.[24] As could be seen from Figure 3g,h, the heating resulted in the crystallization and sublimation of the SiN membrane near the hole starting at 300 µA. The crystallization temperature of the SiN membrane was >1400 °C, which was an indicator for significantly higher temperatures reached by this current annealing.[25] These results show that after the initial carbonization, further graphinization could be achieved by current annealing with a structural evolution comparable to thermal annealing.
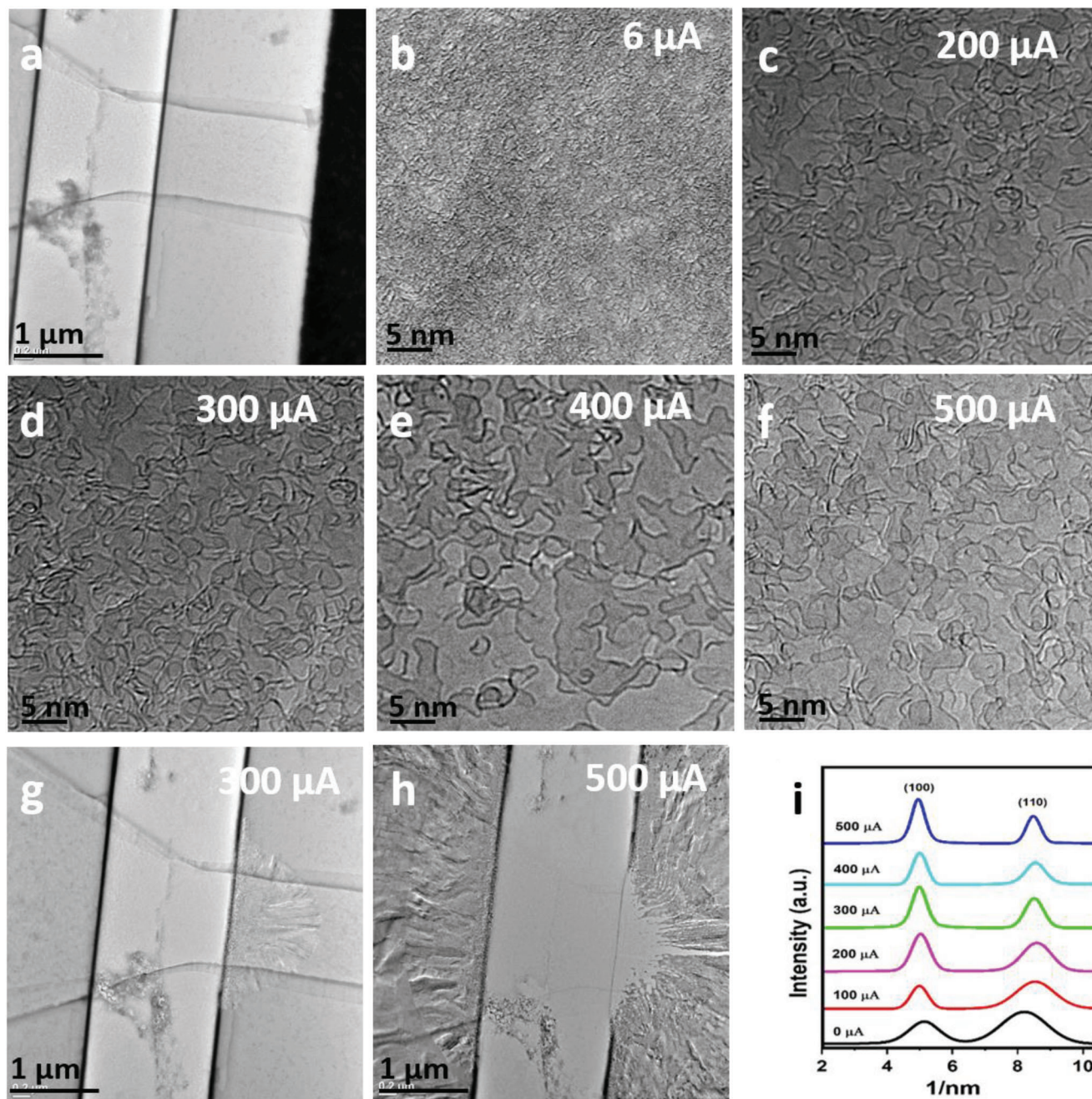
**ADVANCED
SCIENCE NEWS**

www.advancedsciencenews.com

Macro-
olecular
Materials and Engineering
Open Access

www.mame-journal.de

Figure 3. a) Patterned ncg before current annealing. b) Structure at the start of current annealing. c–f) Evolution of ncg domains during current annealing. g,h) Crystallization of the SiN membrane near the edge and i) evolution of SAED intensity profile.

This provided the possibility to locally control the crystallite size by current annealing. Apart from control over the crystallite size, current annealing allowed to directly follow the resistance evolution (Figure S3, Supporting Information) and thus provided an opportunity for direct tailoring of the electrical response. The data recorded during the in situ measurement showed that the dissipated power and hence the temperature increases in a controlled fashion linearly with increasing current. This results point to new possibilities to tailor the structure and conductivity of pyrolyzed polymer thin films by current annealing.

To investigate the structural changes at even higher temperatures, current annealing was carried out on a similar sample and the annealing current was increased beyond 500 µA. With increasing temperature, the crystallite size increased further and the sample eventually broke at a current of 800 µA. The broken thin film after current annealing could be seen in **Figure 4**. The images show the presence of distributed graphene flakes on top of a thin extended few layers graphene film. Unlike the early stages of pyrolysis, the flakes were large and exhibit defined shapes. Some graphene nanoflake residues could also
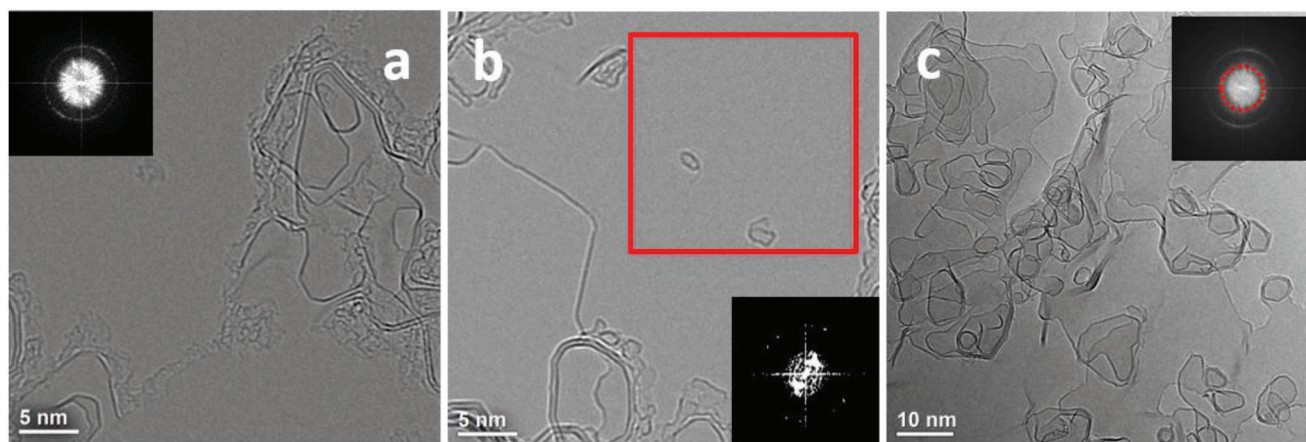
Figure 4. a) Nominally 1 nm thick film after current annealing to high temperatures, showing the presence of large domains and the FFT showing one ring corresponding to the (100) planes in carbon. These large structures are distributed over graphenized layers formed during current annealing. We can also see some residues on the top of the layers that are not fully grown yet. b) Large area showing a few discrete spots in the FFT, corresponding to highly grown crystallites. c) Slightly thicker region with the FFT showing an additional ring corresponding to the (002) planes indicating the presence of stacking of layers perpendicular to the substrate.

be observed which have not completely grown yet. Figure 4b showed a large thin film area with only a few nano structures distributed on top of it. The FFT from an area of ≈20 nm² showed only a few discrete spots, which was an indication that the structure has grown considerably from the average crystallite size of 3.2 nm reached by thermal annealing during current annealing.[24] Furthermore, it should be noted that the FFT in Figure 4a only showed one ring corresponding to (100) planes, representing an in-plane growth of these thin films with the graphene layers parallel to the substrate. It was to be noted that the layers were orienting parallelly and the graphene units in the parallel layers did not show preferential alignment within the planes. This could lead to the formation of more extensive polycrystalline graphitic domains at higher temperatures by oriented attachment of domains and Ostwald-like ripening as shown in the previous studies.[13,24] Current results confirm the possibility to push polymer thin film pyrolysis beyond the nanocrystalline regime to the formation of (few layer) graphene.

Apart from the thin regions, there were also some thick regions observed in the sample. This variation in thickness could be due to the conversion of the carbonaceous residues from the lithography process. These residues could convert and grow to graphene nano flakes on the top of the nano graphene layers, increasing the thickness. Looking at a thicker region, (Figure 4c), the FFT showed a diffuse ring corresponding to the (002) planes in graphite lattice indicating the presence of vertical stacking of graphene layers in this part of the sample. This is an indication for a dependence of the ordering and growth of crystallites. To understand the thickness effects for the graphitization and the structural evolution, current annealing experiments were conducted for thicker samples (≈10 nm) as shown in **Figures 5** and **6**. Graphenization and growth could be confirmed from the images and SAED patterns in Figure 5a–d. The two rings 0.12 and 0.21 nm⁻¹ in the patterns corresponded to the (100) and (110) planes showing in-plane oriented graphene. With increasing annealing current, there was a sudden change in the structure at 800 µA. The structure transforms to large multi-walled cage-like structures,

resembling bamboo-type MWCNTs with a strong 002 diffraction ring corresponding to a turbostratic interlayer distance. The size of these cage-like structures was ≈40 to 50 nm. The cage-like structures showed a directional elongation toward the electrodes. This could be due to the stress induced in the film due to the negative coefficient of thermal expansion of the graphitized films[26] or because of electro-migration during heating and transformation. More detailed studies would be necessary to understand the mechanism behind the observed directional growth. In addition, some metallic particles could be observed in the images, as well as some corresponding additional reflections in the SAED patterns. The metallic impurities were due to the platinum electrodes of the MEMS-based chip melting at a current of 800 µA (melting point 1768 °C), leading to individual Pt nanoparticles electro-migrating along with the current through the sample. The Video S1 (Supporting Information) showed the migration of the platinum electrode over the graphitized sample.

The current annealed region of a similar thick sample provided further insights into these stacked structures (Figure 6). The cage-like structures were not discrete, but are fused and well-connected. A well-defined graphene layer stacking could be seen in Figure 6a–d with the FFT from the area marked shown in Figure 6g. The FFT shows two sets of spots corresponding to 0.344 and 0.210 nm corresponding to (002) and (100) reflections in graphite. The 0.344 nm corresponded to the interlayer distance in turbostratic interlayer distance and gives the indication of vertical stacking in the thick sample. In both samples, the formation of these cage-like structures was rapid.

Previous studies on current annealing of few layers of graphene showed bonding of adjacent layers to form bonded bilayers with increased stability compared to the open unsaturated edges.[27] The reported structural transformation during current annealing of the thick samples was different. In case of bulk graphite, current annealing resulted in the formation of aligned hollow 3D shells bound by a few layers of graphene.[20] Transformation of folded bilayers to hollow structures during
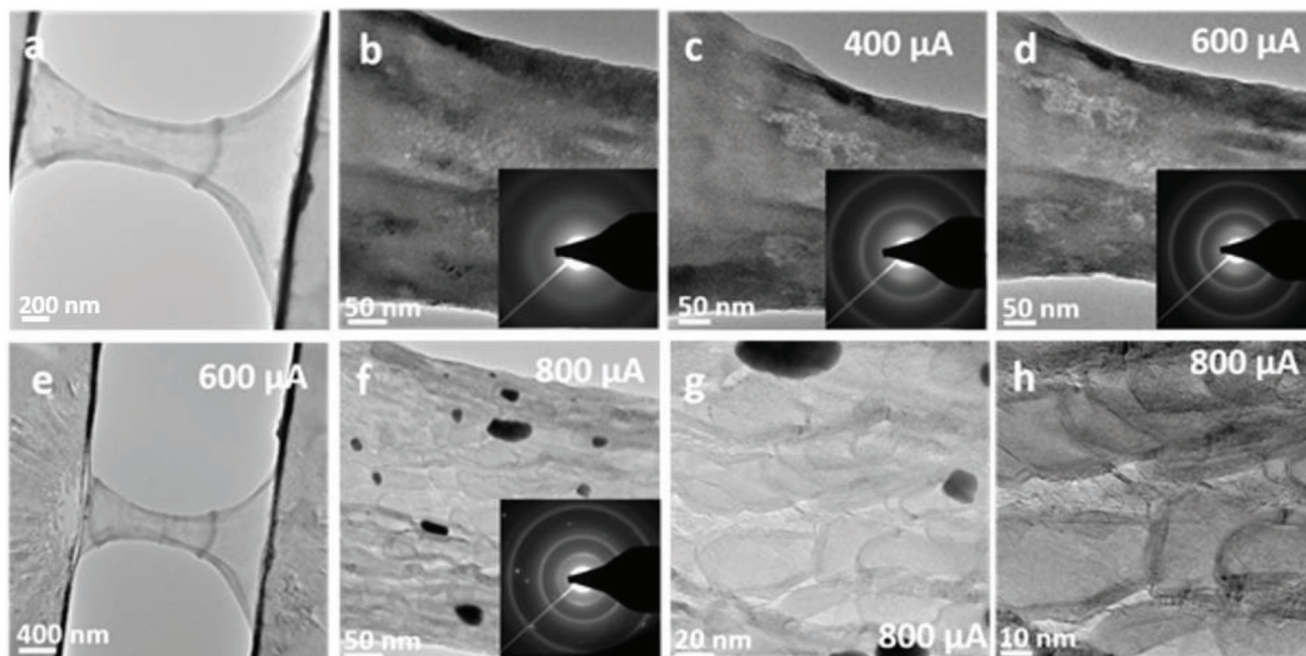
**ADVANCED
SCIENCE NEWS**

www.advancedsciencenews.com

**Macro-
molecular
Materials and Engineering**

www.mame-journal.de

Figure 5. Current annealing of a thick sample. a) Sample before current annealing. b–d) Growth of domains during current annealing. e) Crystallization of the SiN membrane on both sides of the hole f–h) highly grown multi-walled cage-like structures.

passage of current was the proposed mechanism.[18] In the case of amorphous carbon fibers, stacked tubular structures were reported during in situ current annealing inside a TEM.[19] It was reported that the tubule formation is through diffusion, which was active at high temperatures. However, during in situ heating of thin samples, migration and merging of graphene nano flake was the dominant mechanism resulting in the oriented growth of the thin film.[13,24]

These results show that there is a difference in structural evolution during the pyrolysis of thin and thicker structures. Thin films exhibit almost exclusive growth of highly oriented layers with the possibility to completely graphitize the film at high temperatures. On the other hand, thicker samples result in the formation of cage-like structures. Even though S1805 is considered a graphitizable precursor at low thickness,[1,4,10] the formation of cage-like structures was observed that were stable and resulted in the formation of a non-graphitizing glassy carbon at this intermediate thickness. At lower thicknesses carbons preferentially align parallelly, which increases the graphitzability and leads to the formation of completely graphitized carbon at sufficiently high temperatures/currents. On the other hand, at intermediate thicknesses, unsaturated bonds plays a critical role and result in bending and the formation of cage-like structures.

This critical effect of the sample thickness was confirmed, by investigating the graphitization of SU8 thin films. SU8 is normally considered a non-graphitizing polymer and only forms glassy carbon structures during carbonization in the bulk.[2,28] However, when heated in situ to 1200 °C a nominally 1 nm thin SU8 film shows a similar structural evolution as S1805, mostly consisting of well-aligned graphitic layers (**Figure 7**). This also fits to previous studies on in situ heating of SU8 films, where at the thin edge of the sample well aligned ncg flakes were observed,

whereas thicker areas exhibit a typical glassy carbon structure with multi-walled cage-like features.[14]

The combination of the results from both precursors forming highly aligned few layers graphene from thin polymer films and cage-like structures similar to glassy carbons at intermediate thickness clearly demonstrate the general critical role of film thickness during carbonization.

3.2. Understanding the Effect of Thickness on Growth and Graphitizability

To develop an atomistic understanding of the underlying mechanisms, molecular dynamic simulations were carried out to understand the effect of thickness on graphitization and the dynamics behind the formation of the cage-like structures. MD simulations were carried out starting from amorphous carbon structures with varying thickness. **Figure 8** shows the orientation of carbon atoms for different thickness during annealing (as defined in the Experimental Section). The atoms with angles close to zero were oriented parallel to the surface and the misorientation increased with increasing angle. Figure 8a represents the structural changes after annealing a 35 Å thick film, which forms well aligned 9 layers of graphene (see Figure S1, Supporting Information). When the thickness was increased, only the graphene layers close to the surface were well aligned (≈3–5 graphene layers), while the orientation of the layers changed in the central region of the film. These misoriented domains were stable for the time scale accessible in the MD simulations (here 1000 ps, see also Figure 8d), preventing the formation of uniformly oriented graphene layers, even in the high-temperature regime of 3500 K (see Video S2, Supporting Information). The simulation
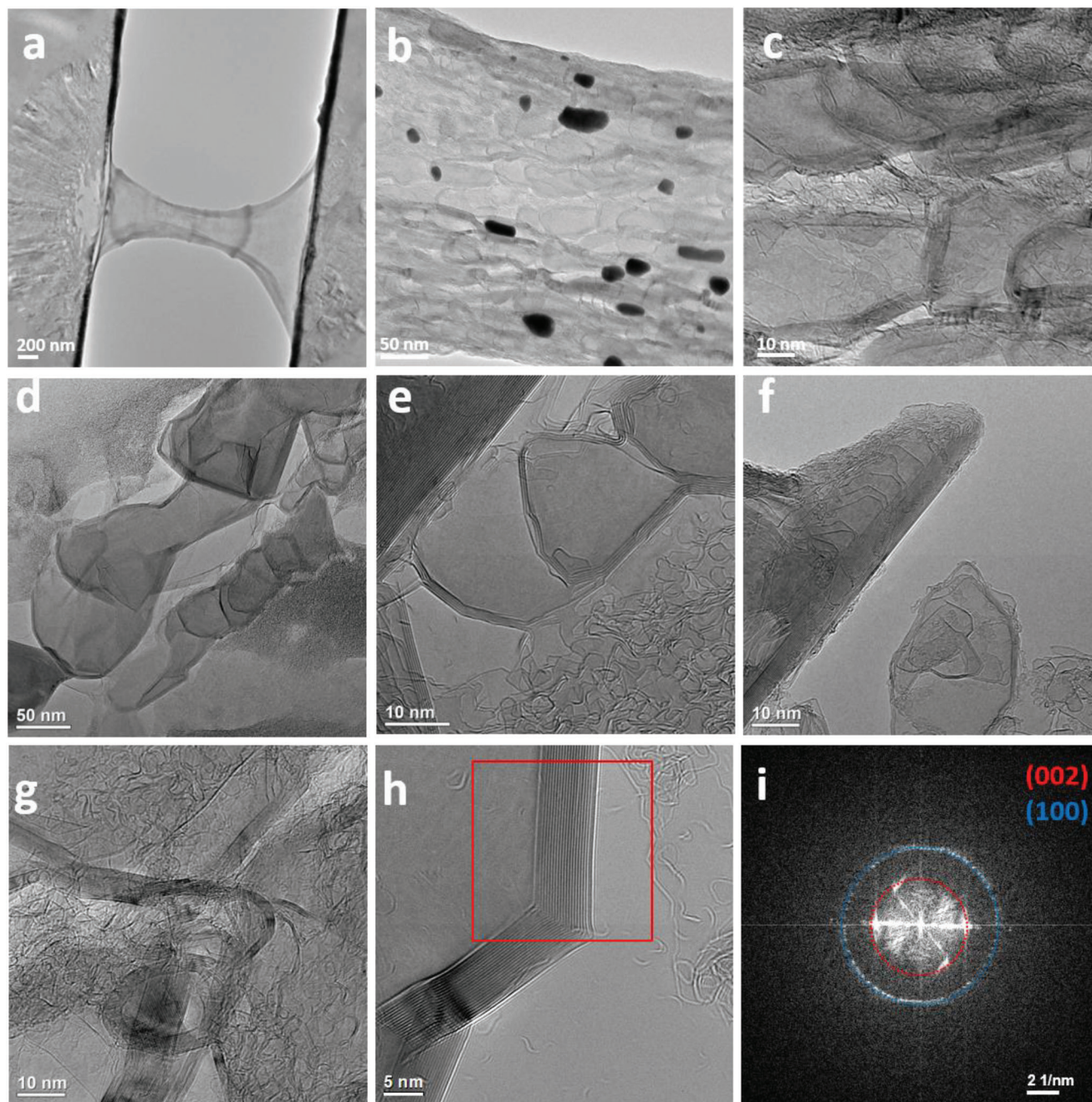
Figure 6. a–d) Interconnected cage-like structures observed in the thick sample. e–g) Well stacked walls of a cage-like structure and i) FFT from the marked region in h) showing two sets of diffraction spots corresponding to 002 and 100 reflections.

temperature was higher than the experimentally calculated temperature. Higher temperature was used to see if there in any difference in the experimentally observed structural changes at high temperatures. This agrees with the observed structural evolution in the thin films, which showed extended domains with a strongly preferred in-plane growth orientation for the nominally 1 nm thick film and cage-like structured for the nominally 10 nm thick film. These experimental and simulation results provide new information on the effect of thickness during graphitization. Within the limit of the MD simulations, a thickness of ≈40 Å

could be determined, below which alignment of the domains is fast and uniform throughout the sample. It is believed that at this low thickness, the surface effects are strong enough to enforce the whole structure to align parallel to the surface. As the thickness increases, ordering of the crystallites becomes more and more difficult leading to the misoriented structure.

The effects leading to the formation of cage-like structures were further examined in simulations of smaller systems with activated edges. The edges were activated by slicing (i.e., removing some atoms from the layered structure). As could be seen
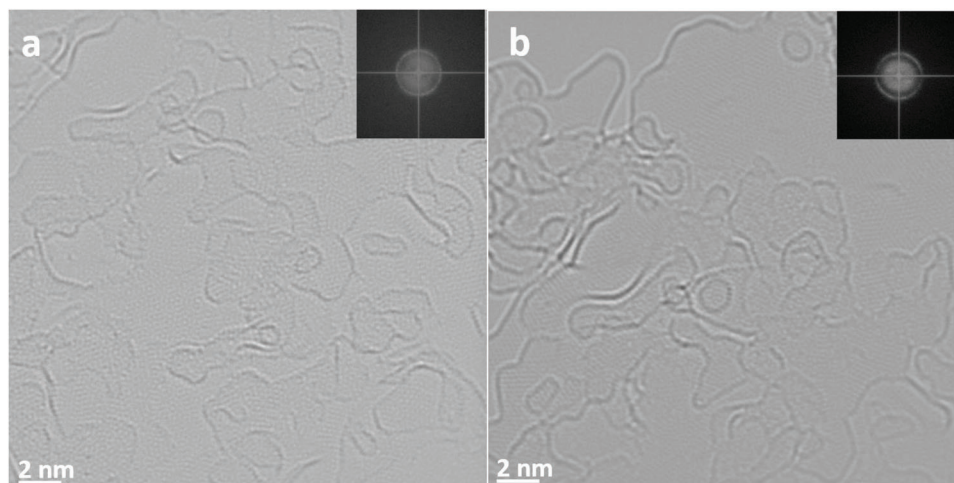
ADVANCED
SCIENCE NEWS
www.advancedsciencenews.com

macro-
molecular
Materials and Engineering
Open Access
www.mame-journal.de

Figure 7. a,b) HRTEM Images of thin regions of SU8 heated to 1200 °C. The corresponding FFT shows only one ring corresponding to the (100). The structure is similar to the ones observed for S1805 in previous studies.[13,24]
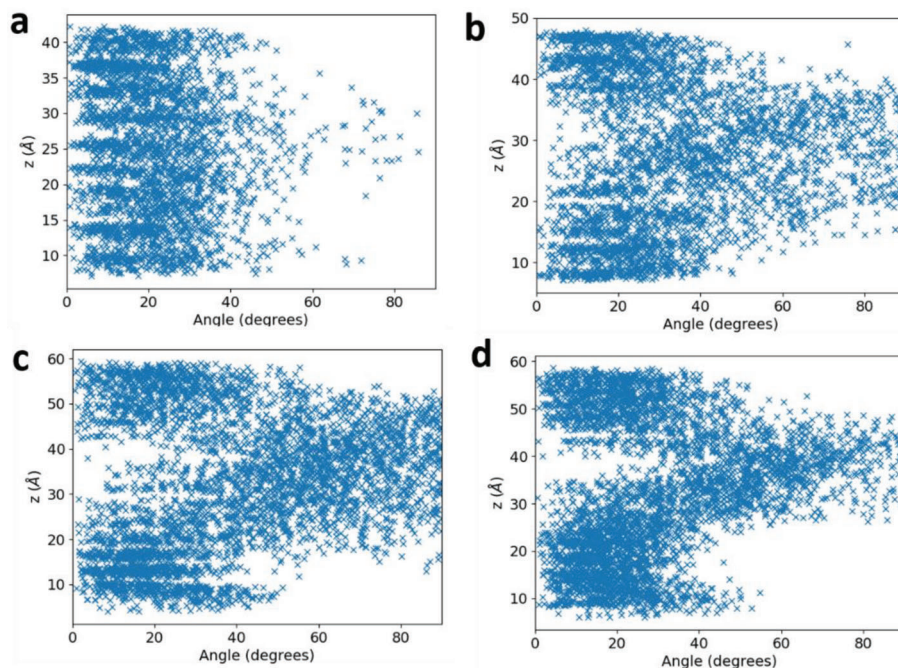

Figure 8. Effect of thickness on the ordering of crystallites. Snapshots after 420 ps for an initial layer thickness of a) 35 Å (≈3100 carbon atoms, depicted as blue crosses) and b) 40 Å (≈3600 atoms). Snapshots for an initial layer thickness of 50 Å (≈4500 atoms) after c) 220 and d) 1020 ps. For the 35 Å sample, the structure is aligned with the surface (angles close to 0°) and forms 9 almost parallel graphene layers during annealing. For thicker samples, the number of misoriented atoms increases toward the center of the film.

in **Figure 9** and Video S3 (Supporting Information), the active edges are highly reactive and directly start to form bonds with surrounding atoms. It is interesting to note that initially bonds were formed with atoms in directly neighboring layers (bonded bilayers), but these are not stable and form multi-layer cage- or tube-like structures afterward. In other words, the bonds with the directly neighboring layers are only an intermediate step to start bending and thus the formation of bonds with layers further away, which are thermodynamically more favorable. As soon as the multilayer structures were formed, they were stable dur-

ing the remaining simulation time (here ≈300 ps). Depending on the aspect ratio of the cross-section after slicing and whether the number of layers that could be formed is even or odd, multi-layer nanotubes or multilayers with passivated edges can form. As could be seen in Figure 9, starting from a 15 Å thick and 30 Å wide carbon stack (with periodic boundary conditions along one in-plane direction) a bilayer carbon nanotube was formed. Intermediate steps were the creation of active edges via slicing (i.e., removing atoms to form a 1D periodic structure; Figure 9b) followed by the formation of bonds between neighboring atoms
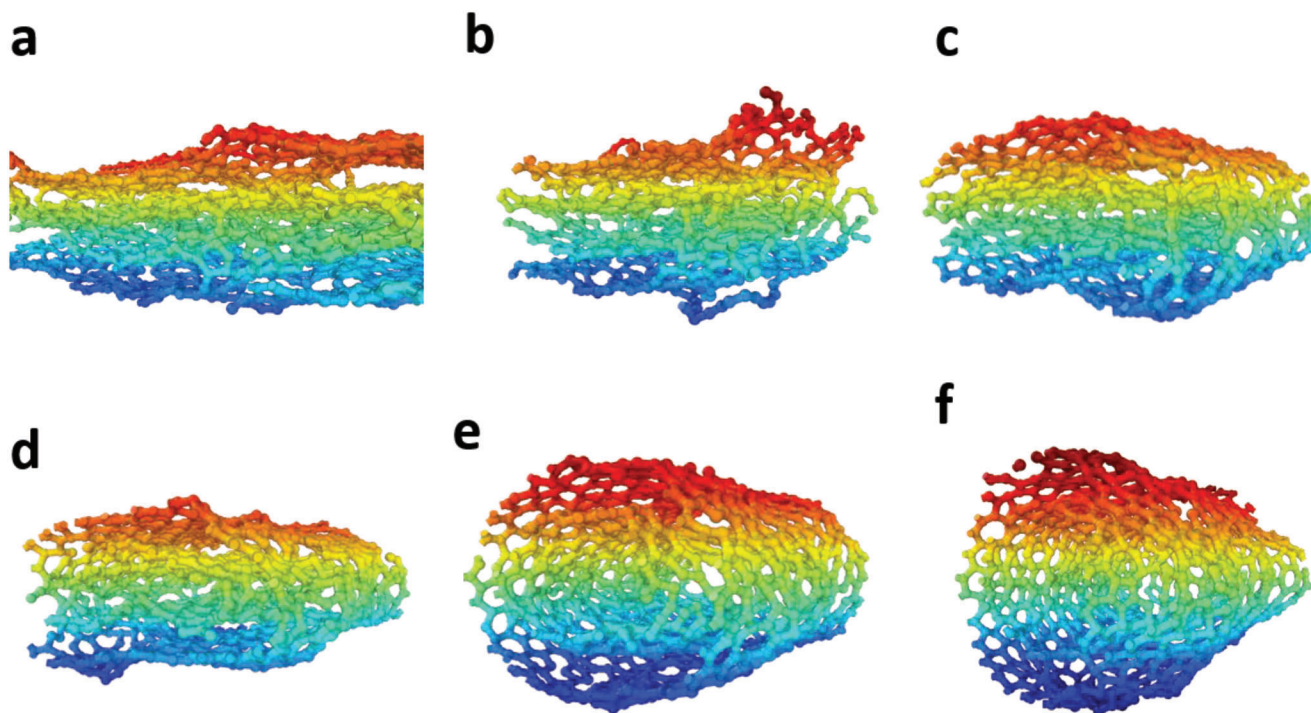
ADVANCED
SCIENCE NEWS

www.advancedsciencenews.com

acro-
olecular
Materials and Engineering
Open Access

www.mame-journal.de

Figure 9. Formation of cage-like structures from bonded multi-layers: a) initial structure after equilibration (120 ps): 4 graphene layers, periodic in length and breadth. b) Structure directly after slicing (121 ps): active edges. c) Edge passivation (144 ps): here bonds are formed between directly neighboring layers. d) Bilayer formation (164 ps): temporary bonds present in (c) re-align and result in the formation of bilayer edges. e) Nanotube formation (224 ps): depending on the cross-section geometry, the bilayer structure can transform into a nanotube (here) or a flat cage-like structure similar to the one in (d). f) Final structure (520 ps): stable bilayer carbon nanotube. For better visualization the atoms are colored coded depending on their height in the film. The corresponding video is available in Video S4 (Supporting Information).

(Figure 9c). This intermediate state of single-layer walls between neighboring layers was unstable due to the high bending at the edges. Thus, it transformed to a multi-wall structure via rearrangement of the bonds connecting the layers (Figure 9d). The bilayer structure then relaxes to a bilayer carbon nanotube, decreasing the energy of the highly bent edges (Figure 9e,f). In the shown example, the number of initial layers was even, so a multi-wall carbon nanotube can form. With an odd number of initial layers, the final structure is a flat multi-wall structure since relaxation to the circular cross-section is prevented by the middle layer. Video S3 (Supporting Information) of a structure with 40 Å thickness is an example for this flat graphenic multilayer structure. Similar cage-like structures can be observed in center of the sample described in the Figure 8 (Video S2, Supporting Information). This explains that the formation of multiwalled cage-like structures is initiated from the active edges and a reduction in energy by reducing the curvature of the edges. This formation can be more favorable with increasing thickness since the edge curvature can reduce with increasing number of layers.

These experimental and simulation results clearly show the effect of thickness on the microstructural evolution and, more important, the graphitizability during pyrolysis at small length scales. When the thickness was lower, the films could grow and align completely leading, to a graphitized carbon with extended oriented domains. When the thickness was increased, the misorientation increases and results in the formation of multi-walled cage-like structures. Once formed, these cage-like structures sta-

ble, even at simulated annealing temperatures of 3500 K corresponding to a non-graphitizing structure. This stability could be explained with the observed formation of bonded multi-walled structures from the primary activated edges.

It should be noted that the multi-walled cage-like structures observed here are similar to the fullerene-related model proposed for commercial glassy carbons.[29] Thus, the current understanding of the formation and stability of close caged structures may provide new insights for the structural evolution in bulk glassy carbon, its low density and more importantly, the non-graphitizing nature of it.

4. Conclusion

Using in situ current annealing in a TEM combined with MD simulations, we investigated the structural evolution and thickness effects during carbonization of polymer thin films. The structural evolution during current annealing was similar to the evolution during thermal heating reported previously. At high currents (temperatures), the thin polymer films were converted to large aligned graphene films consisting of a few highly aligned graphene layers. In contrast, thicker polymer precursors showed a conversion to multi-walled cage-like structures. This behavior was experimentally observed both for S1805 and SU8, suggesting that the film thickness dominates this transition between the two graphitization modes. MD simulations indicate that at lower thickness, <40 Å, the layers tend to order forming well

aligned layers. For thicker samples, the first 4–5 graphene layers are aligned with the substrate, whereas the structure becomes increasingly misoriented toward the middle of the film. This cage-like structure was stable even during simulated annealing at high temperatures of 3500 K explaining the formation of stable glassy carbon structures. This stability can be explained by the formation of bonded multi-layers from the initially highly reactive edges of graphene flakes. The formation of the cage-like structures proceeds via bending of the layers, initially by bond formation between neighboring layers resulting in the formation bonded bilayers as an intermediate structure. Further rearrangement quickly leads to the formation of the highly stable multi-walled cage-like structures. The experimental work and the simulation studies provide new insights into the structural evolution during pyrolysis and the effect of thickness on the graphitizablity in thin polymer films.

Supporting Information

Supporting Information is available from the Wiley Online Library or from the author.

Conflict of Interest

The authors declare no conflict of interest.

Data Availability Statement

The data that support the findings of this study are openly available in KI-Topen at https://doi.org/10.35097/1606, reference number 1000159975.

[1] Q. Zhang, L. Tang, J. Luo, J. Zhang, X. Wang, D. Li, Y. Yao, Z. Zhang, *Carbon* **2017**, *111*, 1.
[2] S. Sharma, *Materials* **2018**, *11*, 1857.
[3] L. Zhang, Z. Shi, Y. Wang, R. Yang, D. Shi, G. Zhang, *Nano Res.* **2011**, *4*, 315.
[4] A. Riaz, F. Pyatkov, A. Alam, S. Dehm, A. Felten, V. S. K. Chakravadhanula, B. S. Flavel, C. Kübel, U. Lemmer, R. Krupke, *Nanotechnology* **2015**, *26*, 325202.
[5] S. Sharma, A. M. Rostas, L. Bordonali, N. Mackinnon, S. Weber, J. G. Korvink, *J. Appl. Phys.* **2016**, *120*, 235107.
[6] R. E. Franklin, *Proc. R. Soc. A* **1951**, *209*, 196.
[7] G. M. Jenkins, K. Kawamura, *Nature* **1971**, *231*, 175.
[8] L. L. Ban, D. Crawford, H. Marsh, *J. Appl. Crystallogr.* **1975**, *8*, 415.
[9] P. J. F. Harris, *J. Mater. Sci.* **2013**, *48*, 565.
[10] Z. Zhang, Y. Guo, X. Wang, D. Li, F. Wang, S. Xie, *Adv. Funct. Mater.* **2014**, *24*, 835.
[11] S. Sharma, A. Khalajhedayati, T. J. Rupert, M. J. Madou, *ECS Trans.* **2014**, *61*, 75.
[12] S. Sharma, A. Sharma, Y.-K. Cho, M. Madou, *ACS Appl. Mater. Interfaces* **2012**, *4*, 34.
[13] C. N. S. Kumar, M. Konrad, V. S. K. Chakravadhanula, S. Dehm, D. Wang, W. Wenzel, R. Krupke, C. Kübel, *Nanoscale Adv.* **2019**, *1*, 2485.
[14] S. Sharma, C. N. Shyam Kumar, J. G. Korvink, C. Kübel, *Sci. Rep.* **2018**, *8*, 16282.
[15] A. Barreiro, F. Börrnert, S. M. Avdoshenko, B. Rellinghaus, G. Cuniberti, M. H. Rümmeli, L. M. K. Vandersypen, *Sci. Rep.* **2013**, *3*, 1115.
[16] B. Westenfelder, J. C. Meyer, J. Biskupek, S. Kurasch, F. Scholz, C. E. Krill, U. Kaiser, *Nano Lett.* **2011**, *11*, 5123.
[17] G. Yang, L. Li, W. B. Lee, M. C. Ng, *Sci. Technol. Adv. Mater.* **2018**, *19*, 613.
[18] P. J. F. Harris, *Carbon* **2012**, *50*, 3195.
[19] J. Y. Huang, S. Chen, Z. F. Ren, G. Chen, M. S. Dresselhaus, *Nano Lett.* **2006**, *6*, 1699.
[20] P. J. F. Harris, *Carbon* **2016**, *107*, 132.
[21] S. Plimpton, *J. Comput. Phys.* **1995**, *117*, 1.
[22] C. De Tomas, I. Suarez-Martinez, N. A. Marks, *Carbon* **2016**, *109*, 681.
[23] H. M. Aktulga, J. C. Fogarty, S. A. Pandit, A. Y. Grama, *Parallel Comput.* **2012**, *38*, 245.
[24] C. N. Shyam Kumar, V. S. K. Chakravadhanula, A. Riaz, S. Dehm, D. Wang, X. Mu, B. Flavel, R. Krupke, C. Kübel, *Nanoscale* **2017**, *9*, 12835.
[25] H. Schmidt, W. Gruber, G. Borchardt, M. Bruns, M. Rudolphi, H. Baumann, *Thin Solid Films* **2004**, *450*, 346.
[26] D. Yoon, Y.-W. Son, H. Cheong, *Nano Lett.* **2011**, *11*, 3227.
[27] J. Y. Huang, F. Ding, B. I. Yakobson, P. Lu, L. Qi, J. Li, *Proc. Natl. Acad. Sci. USA* **2009**, *106*, 10103.
[28] S. Sharma, M. Madou, *Bioinspired, Biomimetic Nanobiomater.* **2012**, *1*, 252.
[29] P. J. F. Harris, *Philos. Mag.* **2004**, *84*, 3159.